journal

J. Am. Ceram. Soc., 77 [10] 2712–20 (1994)

Active Brazing Alloy Containing Carbon Fibers for Metal–Ceramic Joining

Mingguang Zhu and D. D. L. Chung

Composite Materials Research Laboratory, State University of New York, Buffalo, New York 14260-4400

The addition of 8.4 vol% short metal-coated carbon fibers to an active brazing alloy increased the debonding strength of metal/ceramic joints by 18% to 28%. The carbon fibers helped to strengthen the brazing alloy and to decrease slightly the thermal stress at the brazing interface. The carbon fibers were either uniformly distributed in the brazing layer or concentrated near the ceramic side of the metal/ceramic brazing interface. The latter resulted in a lower thermal expansion in the part of the brazing filler near the ceramic and gave superior joints such that the debonding occurred in the part of the brazing filler without carbon fibers. The titanium in the active brazing alloy was segregated at the interfaces between the brazing filler and the ceramic, between the brazing filler and the metal (steel), and between the carbon fibers and the matrix of the brazing filler. The amount of titanium at the interface between the brazing filler and the ceramic was smaller when carbon fibers were present in the brazing filler. Titanium segregation at the fiber–matrix interface was also observed when bare carbon fibers instead of metal-coated fibers were used. The bare carbon fibers gave joints comparable in quality to the metal-coated carbon fibers. The carbon fibers also served to lower the cost of the brazing material.

I. Introduction

METAL–CERAMIC joining is involved in electronic packaging, engines, turbines, and numerous other applications that utilize ceramics. Brazing is a widely used joining method, but metal–ceramic brazing has long been a difficult task. First, this difficulty is due to the difficulty of the brazing alloy melt to wet the ceramic surface during the brazing operation. Second, it is due to the difference in thermal expansion coefficient (CTE) between the metal and ceramic being joined.[1–3] Third, it is due to the difference in the CTE between the ceramic and the filler metal. To alleviate the wetting problem, the metallization of the ceramic surface prior to brazing is viable, but it adds an expensive step to the overall process. The use of titanium-containing brazing alloys (called active brazing alloys) can also alleviate the wetting problem.[4] To alleviate the problem of thermal expansion mismatch between the ceramic and the filler metal, the filler metal is preferably thin and ductile; furthermore, carbon fibers may be added to the filler metal to form a filler composite of reduced thermal expansion.[5]

Although the direct brazing method using active brazing alloys leads to a simplification in the bonding process by eliminating the need for prior metallization and has potential for high production capability,[6,7] the higher CTE of active brazing alloy compared to those of ceramics still limits its application.[8]

A composite brazing material in the prior art is a composite consisting of a conventional brazing alloy and molybdenum particles, which serve to lower the cost of the brazing material.[9] In contrast, the carbon fibers in this work serve to improve the metal–ceramic brazed joints as well as lowering the cost.

In this work, chopped carbon fibers were added to an active brazing alloy to prepare a low CTE composite brazing material. The carbon fibers were useful for enhancing the debonding shear strength of bonds between ceramics and stainless steel. The titanium from the active brazing alloy was segregated at the ceramic/braze, carbon fiber/braze, and steel/braze interfaces after brazing. The elements in the steel were found in the brazing layer; especially Fe was concentrated at the ceramic/braze interface.

For obtaining stronger brazed joints, the effects of the cooling rate and the sample configuration were also studied in this paper.

Table I. Coefficient of Thermal Expansion of Several Materials (20–600°C)

Material	CTE ($\times 10^{-6}$/°C)
(1) Carbon fiber	−1.6
(2) Al_2O_3	8.5
(3) SiC	4.2
(4) 304 stainless steel	18.4
(5) Ag–Cu brazing alloy (64% Ag–36% Cu)	19.5
(6) #5 + 8.4 vol% C fiber	17.3*

*Estimated value. The modified rule of mixtures, with consideration of the effects of isostatic stress on adjacent phases,[10] was used.

II. Experimental Methods

The brazing alloys used were active brazing alloys in paste and sheet forms. The brazing alloy paste (Type Cusin-1 ABA) was from WESGO Inc. (Belmont, CA) and contained 63 wt% Ag, 34.25 wt% Cu, 1.75 wt% Ti, and 1.0 wt% Sn (the melting

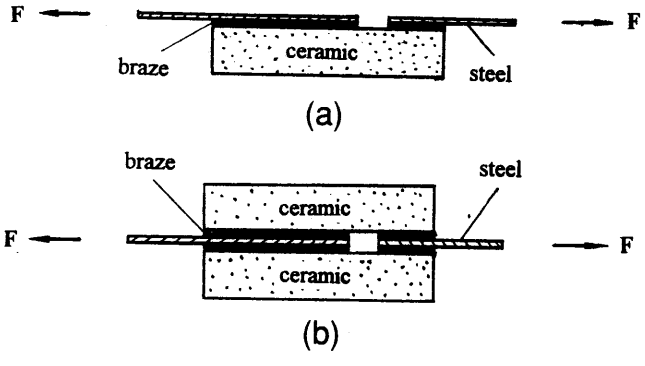

Fig. 1. Sample configurations for mechanical testing under shear: (a) ceramic was bonded only to one side of the steel sheet; (b) ceramic was bonded to both sides of the steel sheet.

R. Loehman—contributing editor

Manuscript No. 194974. Received December 31, 1992; approved March 31, 1993.
This is an extended version of a paper presented at the symposium entitled "Microstructural Design by Solidification Processing" and held at the TMS meeting in Chicago, IL, on November 1–5, 1992.
Supported by the Defense Advanced Research Project Agency of the U.S. Department of Defense and the Center of Electronic and Electrooptic Materials of the State University of New York at Buffalo.

Fig. 2. Polished cross-sectional microstructure of the composite brazing layer between Al_2O_3 (top) and 304 stainless steel (bottom). The carbon fibers were concentrated near the Al_2O_3/braze interface.

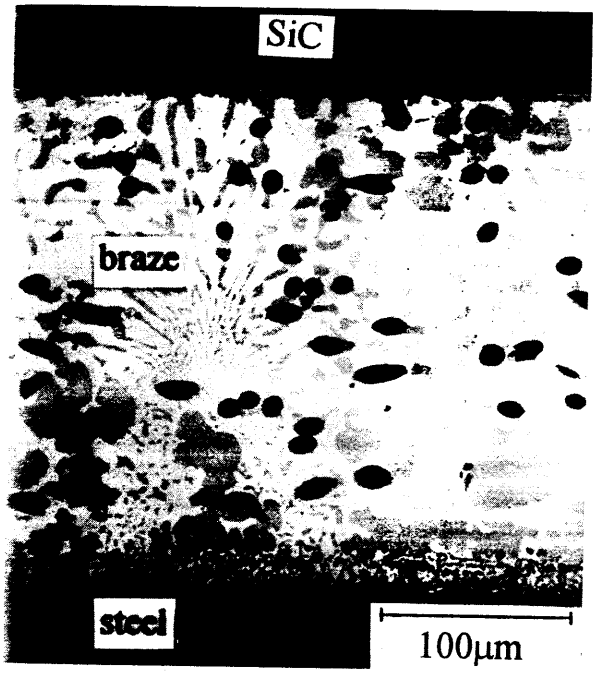

Fig. 3. Polished cross-sectional microstructure of the composite brazing layer between SiC (top) and 304 stainless steel (bottom). The carbon fibers were uniformly distributed.

temperature range of which is 780–815°C). The brazing alloy in sheet form (0.1 mm thick) was CB2 provided by Degussa Metz Metallurgical Corp. (South Plainfield, NJ) and contained 96 wt% Ag–4 wt% Ti (the eutectic temperature of which is 970°C).

The carbon fibers were pitch-based (Thornel P-100 from Amoco Performance Products, Inc.). The continuous fibers of diameter 10 μm were coated with copper (by American Cyanamid Co.) by a plating process. The coated fibers were chopped to lengths of about 500 μm. Each fiber had a copper layer of thickness ~1 μm uniformly covering it.

Two kinds of ceramics were used, namely alumina (Type AL-96 provided by Superior Technical Ceramic Corp.) and silicon carbide (Type Hexoloy SA provided by Carborundum Company). None of the ceramics was polished or metallized prior to brazing.

The chopped carbon fibers were added to the brazing paste and mixed to make a composite brazing paste (containing 8.4 vol% carbon fibers after brazing). The metal used as a component to be joined to the ceramic was 304 stainless steel. The composite brazing paste was applied between the ceramic and the stainless steel. No flux was used during the brazing.

Table I shows the CTE values of several materials. The carbon fiber has nearly zero CTE. The ceramics (SiC and Al_2O_3) also have low CTE values, whereas the CTE of the Ag–Cu brazing alloy is even higher than that of 304 stainless steel. With the addition of 8.4 vol% carbon fibers, the CTE value of the composite brazing filler is between those of the steel and the ceramics, as expected. (Notice that there is no big difference in the CTE value between the steel and the braze.) Yet lower CTE values could be obtained by increasing the carbon fiber volume fraction in the composite brazing filler. However, more carbon fibers would create more interfaces where reaction would occur with the active element (titanium). Since there was limited Ti in the brazing alloy, too many carbon fibers might result in much less active element reacting with the ceramic, thereby weakening the bonding at the ceramic/braze interface. In this work, 8.4 vol% carbon fibers (after brazing) was used to investigate the usefulness of carbon fibers in an active brazing alloy. More investigation is in progress to optimize the carbon fiber content.

By using different proportions of the composite brazing paste and the brazing sheet, the fiber distribution was controlled to make the fibers either uniformly distributed or concentrated near the ceramic side. The joint was heated in a vacuum furnace at a rate of 10°C/min to the brazing temperature (950–1000°C), held at the brazing temperature for 15–20 min, and then cooled at a chosen rate (4.8, 10.6, or 20°C/min). Unless stated otherwise, the cooling rate was 4.8°C/min.

In order to determine the debonding shear strength of ceramic–metal brazements, a modified shear test was developed. The sample configurations are schematically shown in Fig. 1. In one configuration (Fig. 1(a)), the ceramic was bonded only to one side of the steel sheet. In the other configuration (Fig. 1(b)), the ceramic was bonded to both sides of the steel sheet. The latter configuration is preferred since it avoids the bending moment due to the thermal expansion mismatch between the steel and ceramic. Since the steel strip used was thin (0.4 mm), the bending moment in Fig. 1(a) was negligible. In both Figs. 1(a) and (b), the ceramic–steel overlap area was smaller (about 30 mm^2 per side) in the right part than the left part, so that the failure would occur in the right part. The debonding shear strength was calculated from the load at failure and the overlap area.

III. Results and Discussion

(1) Microstructural Design

The design of the braze microstructure involved the following two considerations.

As the carbon fibers have a very low CTE, their graded distribution in the filler metal allows the composite filler metal to have a low thermal expansion near the interface between the ceramic and the composite filler metal and retain its high thermal expansion near the interface between the metal and the filler. From the viewpoint of the thermal stress, a brazing layer with a graded distribution of carbon fibers is preferred.

From another aspect, carbon fibers are a well-known reinforcement in metal–matrix composites.[11] They can also decrease the grain size of the brazing alloy during solidification, as shown by comparing the grain sizes of the top half (with carbon fibers) and the bottom half (without carbon fibers) of the brazing layer in Fig. 2. There is no doubt that, with the addition of carbon fibers, the brazing layer was reinforced. If the interface bonding is strong enough, the part of the brazing layer without carbon fibers could be the weakest part that causes the

Table II. Results of Shear Testing*

Joint	Without carbon fiber		With carbon fiber	
	Strength (MPa)	Crack configuration	Strength (MPa)	Crack configuration
SiC/steel	34.3 ± 8	Cracks were inside the ceramic and parallel to the interface	83.9 ± 2 (Fibers were distributed in the form of a graded junction)	Cracks were inside the ceramic and perpendicular to the interface
Al_2O_3/steel	86.4 ± 3	Cracks were inside the brazing layer	102.1 ± 3 (Fibers were uniformly distributed)	Cracks were inside the brazing layer
			110.7 ± 3 (Fibers were distributed in the form of graded junction)	

*The ceramic was bonded to both sides of the steel sheet. The cooling rate after brazing was 4.8°C/min.

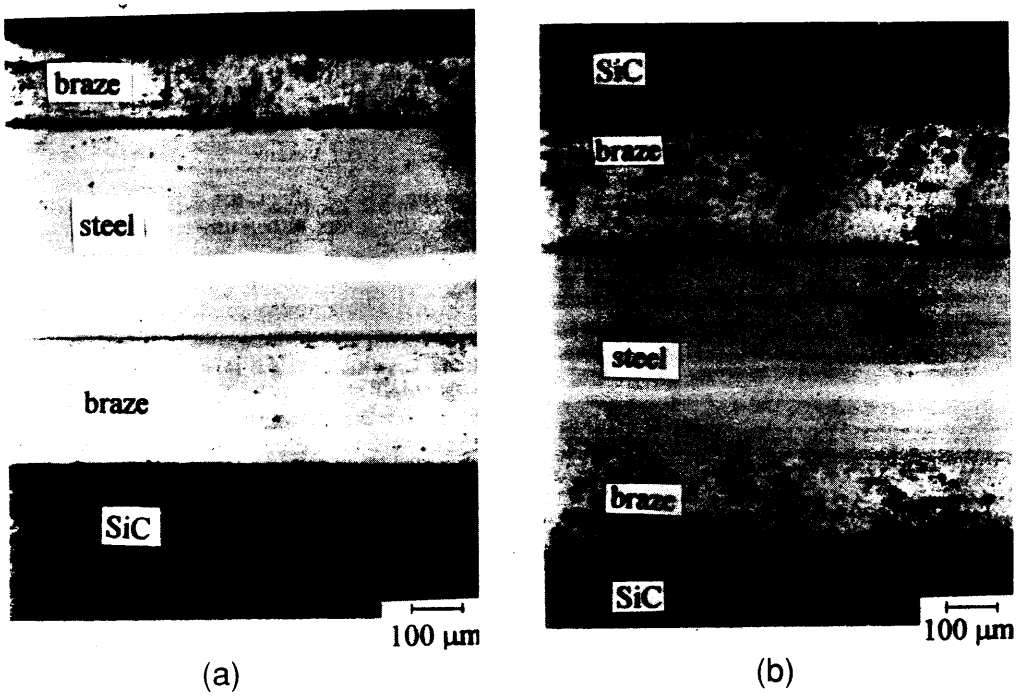

Fig. 4. Polished cross-sectional microstructure of SiC/steel joints after shear testing using sample configuration of Fig. 1(b): (a) Without carbon fibers. Cracks were parallel to the brazing interface. (b) With carbon fibers. Cracks were perpendicular to the brazing interface.

debonding of the joint. Therefore, from the viewpoint of material strength, a brazing layer with uniformly distributed carbon fibers is preferred.

Two cross-sectional microstructural designs of the composite brazing filler were used. In one design (Fig. 2), the carbon fibers were concentrated near the interface between the ceramic and the filler metal, forming a graded junction. In another design (Fig. 3), they were uniformly distributed. The thickness of the brazing layer was 250–350 μm.

(2) Mechanical Testing

Table II shows the results of ceramic/steel debonding testing performed using the sample configuration of Fig. 1(b) and using SiC (3.1 mm thick) and Al_2O_3 (12.7 mm thick) as the ceramics. The cooling rate was 4.8°C/min. At least three samples of each type were tested. For SiC/steel joints, failure occurred inside the ceramic, the cracks were either parallel or perpendicular to the interface for the case without carbon fiber and the case with carbon fiber, respectively. For Al_2O_3/steel joints, failure occurred inside the brazing layer. As the debonding did not occur at the joint interface in SiC/steel joints, the strengths shown in Table II for SiC/steel joints are not the debonding strengths. In contrast, debonding occurred at the joint interface (inside the brazing layer) for Al_2O_3/steel joints, so the strengths shown in Table II for Al_2O_3/steel joints are debonding strengths. For the case of uniformly distributed carbon fibers, debonding occurred at the fiber–matrix interface. For the case of carbon fibers concentrated near the ceramic side, debonding occurred in the part of the brazing layer containing fewer or no fibers. By using carbon fibers that were uniformly distributed, the debonding strength of Al_2O_3/steel joints was increased by 18%; by using carbon fibers that were distributed in the form of a graded junction, the debonding strength of Al_2O_3/steel joints was increased by 28%. Thus, a graded junction resulted in a stronger joint.

Because of the CTE mismatch at the ceramic–metal interface, the residual stress in ceramic/metal joints is large and complex. Suganuna *et al.*[12] used the finite element method to estimate the residual stress of an Si_3N_4/steel joint after it had been cooled from 1000° to 25°C. It was found that the residual stress in the joint was not uniform; near the free surface (edge) and the interface area in the ceramic side, the residual stress was tensile. The tensile stress increased in magnitude as the edge was approached. Our case differs in that a "soft" brazing layer existed between the ceramic and the steel and might cause plastic deformation, which would relieve the thermal stress to some

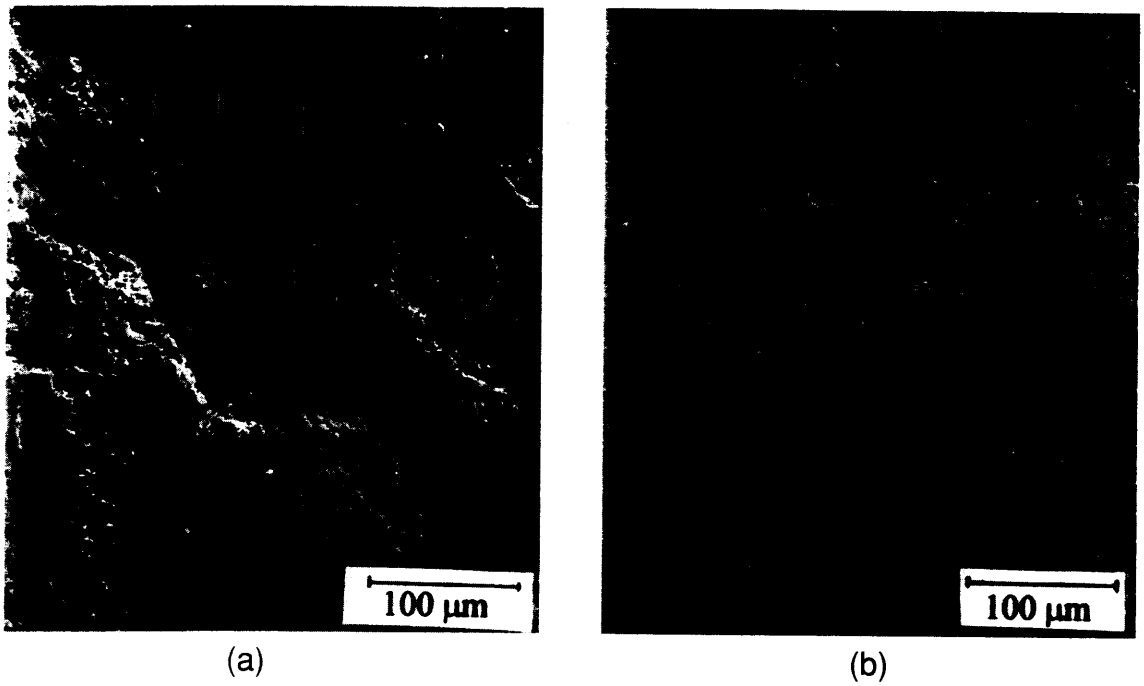

Fig. 5. SEM photographs of the debonding fracture surface of Al_2O_3/steel joint, showing the brazing layer adhered to the Al_2O_3: (a) With carbon fibers. Both microcracks and large cracks were observed on the surface. Fibers were pulled out in the large crack. (b) Without carbon fibers. Microcracks were observed on the surface.

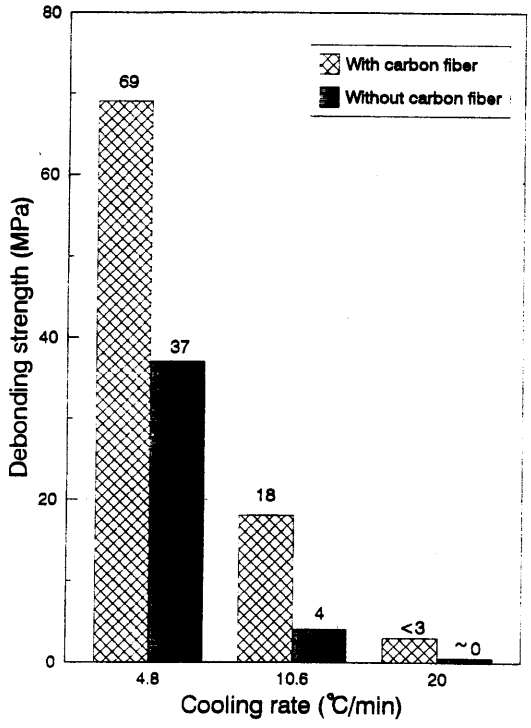

Fig. 6. Effect of the cooling rate on the debonding shear strength obtained using the sample configuration of Fig. 1(a).

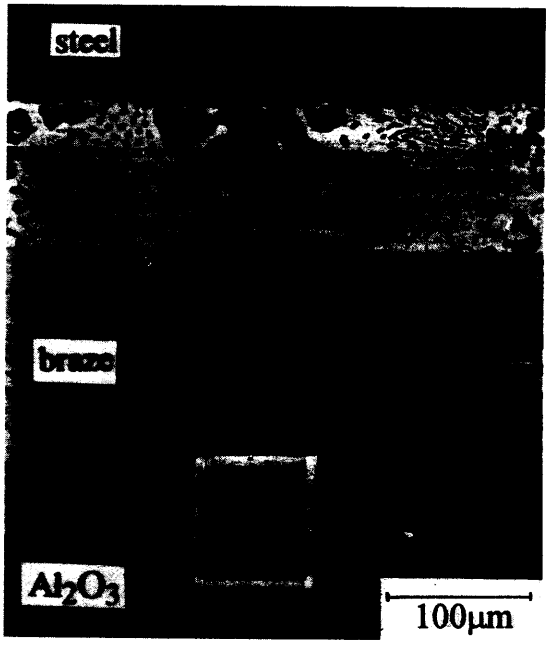

Fig. 7. SEM backscattered electron image of the brazing layer (without carbon fibers).

extent. Nevertheless, the trend of the residual stress distribution should be similar, such that the maximum tensile stress would similarly appear in the corner of the ceramic at the edge of the interface. Therefore, microcracks might initiate in this region during cooling.

For SiC/steel joints, as shown in the bottom of Fig. 4(a), the cracks were parallel to the bonding interface when carbon fibers were not present. It is probably due to the preexisting microcracks (parallel to the bonding interface) that were caused by the thermal stress mentioned above. In contrast, as shown in the bottom of Fig. 4(b), the cracks were perpendicular to the bonding interface when carbon fibers were present. It is thought that, with the help of the carbon fibers, the thermal stress was decreased to the extent that microcracks were not initiated. During the shear test, the applied load resulted in a tensile stress acting on a plane perpendicular to the interface in the ceramic. When the tensile load became high enough, cracks would initiate perpendicular to the interface, causing the breaking of the SiC (of a small thickness of 3.1 mm). The different crack directions in Figs. 4(a) and (b) provide evidence for the fact that the carbon fibers significantly decreased the interfacial thermal stress.

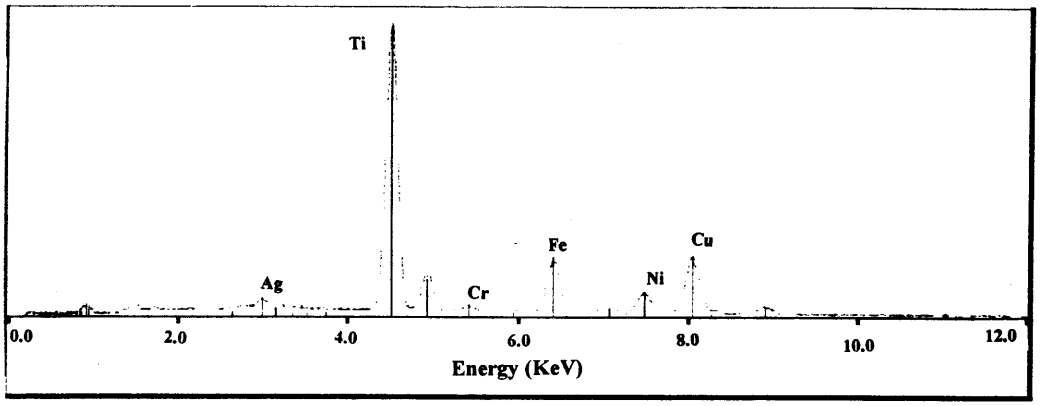

Fig. 8. X-ray spectroscopy analysis of a point at the Al_2O_3/braze interfacial region of Fig. 7.

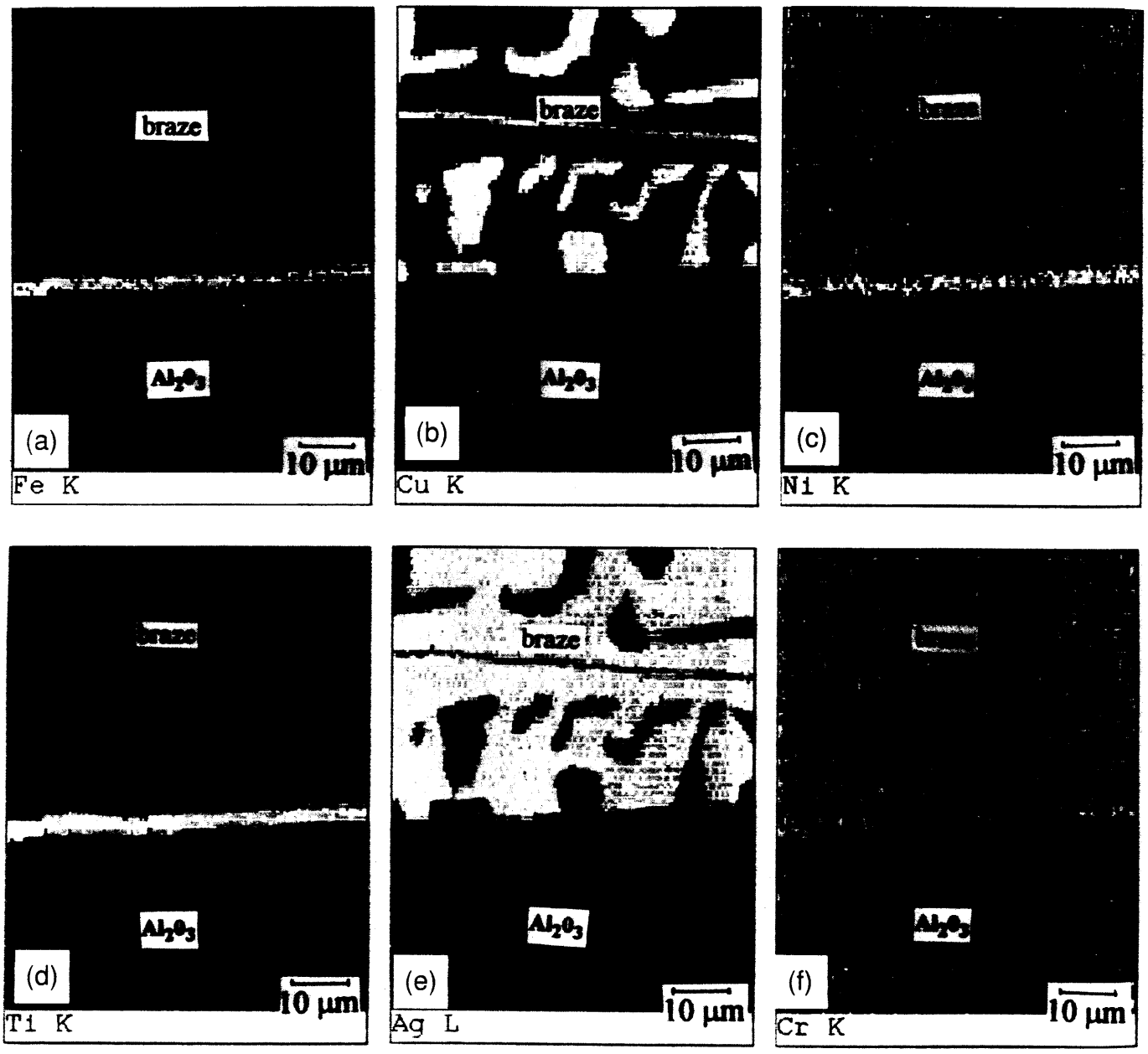

Fig. 9. X-ray maps of the area near the Al_2O_3/braze interface, corresponding to the highlighted region of Fig. 7.

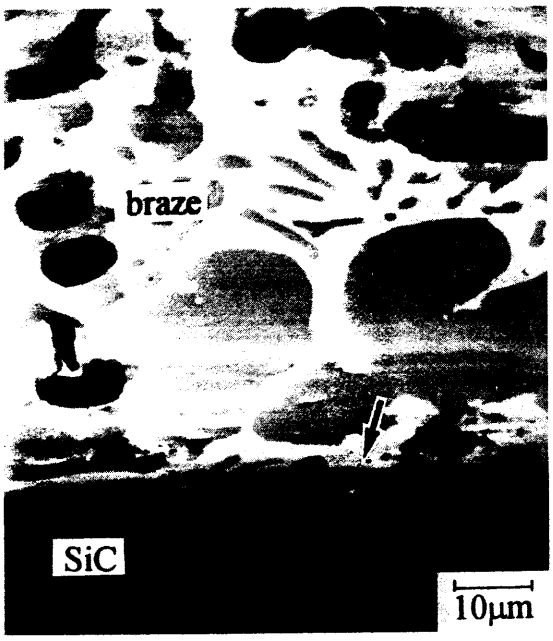

Fig. 10. SEM backscattered electron image of the brazing layer near the SiC/braze interface (with carbon fibers).

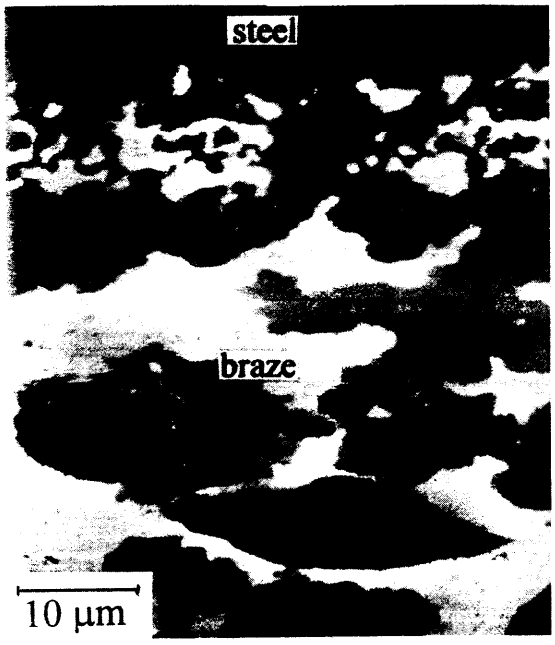

Fig. 11. SEM backscattered electron image of the brazing layer near the steel/braze interface (with carbon fibers).

Figs. 5(a) and (b) are SEM photographs of the Al_2O_3/steel debonding fracture surface, showing the brazing layer adhered to and covering the Al_2O_3 for the cases with carbon fibers (in the form of graded junction) and without carbon fibers, respectively. The steel piece had already been pulled out in the direction from the top to the bottom of each photograph. For the case without fibers (Fig. 5(b)), microcracks were observed in the brazing layer due to the low strength and modulus of the brazing alloy. For the case with fibers (Fig. 5(a)), the fibers were concentrated near the Al_2O_3, which was covered by the brazing layer, and the debonding shear failure occurred in the part of the brazing layer near the steel side, where there was no carbon fiber. This is attributed mainly to the reinforcement of the braze due to the carbon fibers. On the fracture surface, fewer but larger microcracks were observed in the case of Fig. 5(a). The surface of the large cracks was protruded by carbon fibers. These large cracks were a result of the extra resistance against shear at the locations containing carbon fibers. When a sufficiently high shear force was applied and the carbon fibers had been pulled out from the matrix, the steel piece could then move forward and leave behind a large crack. Also we noticed from the crack in Fig. 5(a) that the surface of carbon fibers was smooth; this indicates that the fiber/braze interface was weaker than the fibers or the brazing alloy. By promoting the fiber–matrix reaction, the joint strength may possibly be further increased.

Figure 6 shows the debonding strength obtained by using the sample configuration of Fig. 1(a). Because of the presence of a bending moment after cooling, this sample configuration resulted in a lower debonding strength compared to the sample configuration of Fig. 1(b). An increase of the cooling rate decreased the debonding strength of Al_2O_3/steel joints. As previously mentioned, the main problem in joining metals to ceramics is the thermal expansion mismatch between the ceramic and the metal. The increase of the cooling rate results in more serious thermal stress problem at the joint interface, thus decreasing the debonding strength. With the addition of carbon fibers, which decrease the CTE of the brazing layer, the debonding strength was significantly increased for any cooling rate.

(3) Interface Structure

The interface between the ceramic and the brazing alloy, that between steel and the brazing alloy, and that between a carbon fiber and the brazing alloy are important for understanding the bonding and debonding mechanism of ceramic/steel joints.

An SEM backscattered electron image of a polished cross section of an Al_2O_3/steel brazed joint (without carbon fibers) is shown in Fig. 7. By using X-ray spectroscopy to analyze the chemical composition of the Al_2O_3/braze interface at the center of the highlighted region of Fig. 7, we found that titanium was concentrated at this interface, while iron, chromium, and nickel (the main components of stainless steel) were also found at this interface (Fig. 8).

Figure 9 shows the X-ray elemental maps (for the elements Fe, Cu, Ni, Ti, Ag, and Cr) of the highlighted region of Fig. 7. Figures 10 and 11 are SEM photographs of the microstructure of the SiC/braze and steel/braze interfaces, respectively. The carbon fiber/braze interfaces were also shown in these photographs. Figures 12 and 13 are the X-ray maps of Figs. 10 and 11, respectively. The X-ray maps of Figs. 9(d), 12(f), and 13(d) show that titanium was observed only at the ceramic/braze, steel/braze, and carbon fiber/braze interfaces. Titanium had previously been found to react with ceramics, thus decomposing a layer of the ceramic.[13,14] It has also been found to react with carbon fibers to form a coating on the carbon fibers.[11] From the X-ray maps of Figs. 9, 12, and 13, we can come to a better understanding that titanium plays an important role in the brazing system, as it helps the bonding at each of the three interfaces mentioned above.

Figure 13(a) shows that copper had disappeared from the surface of the originally copper-coated carbon fiber. Instead of copper, titanium (Figs. 12(f), 14(d)), with some chromium (Fig. 12(c)) and silver (Figs. 12(c), 14(e)), composed the fiber/matrix interface. The copper coating helped the wetting of the molten brazing alloy on the fiber. However, the heating caused mass transfer and chemical reaction to occur at the interface. Finally, the copper dissolved in the matrix (an Ag–Cu alloy) and titanium reacted with the carbon fiber and remained at the interface.

Figure 14 shows the braze microstructure near the ceramic (Al_2O_3) side when bare carbon fibers (low-cost isotropic-pitch-based fibers) instead of copper-coated carbon fibers (high-cost mesophase-pitch-based fibers) were used. As in the case of copper-coated carbon fibers, titanium segregation was observed at

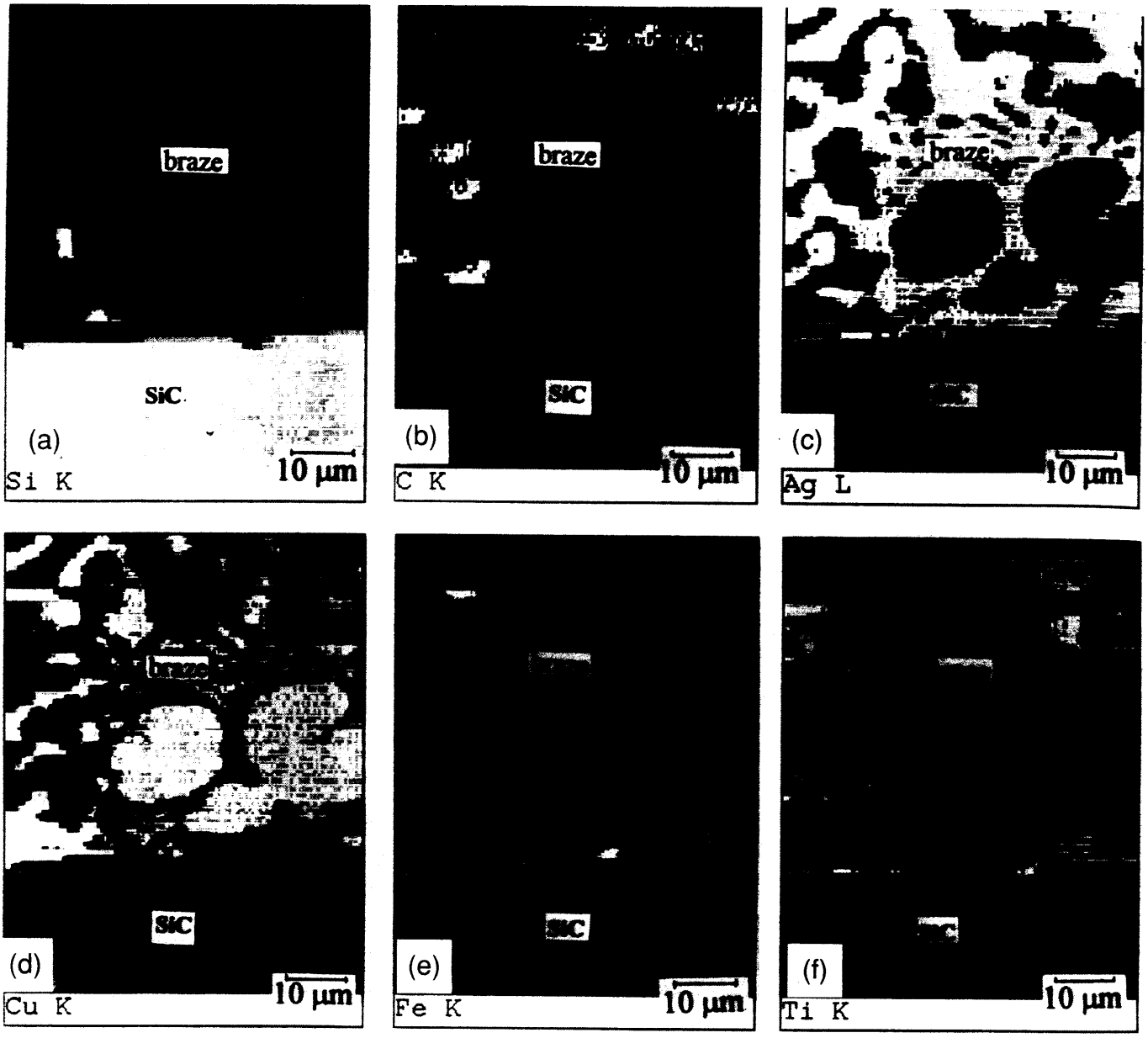

Fig. 12. X-ray maps for several elements in the region shown in Fig. 10.

the interface between the ceramic and the braze. In spite of the absence of a metal coating on the bare carbon fibers, the bare carbon fibers were bound well by the matrix (Fig. 14(a)). Comparison of the carbon fiber cross section in Fig. 11 (copper-coated carbon fibers) and that in Fig. 14 (bare carbon fibers) suggests that the copper coating (plating) process caused some defects in the carbon fibers. Furthermore, the coated fibers are expensive compared to the bare fibers. Although the data given in this paper were obtained using copper-coated carbon fibers, bare carbon fibers provided joints of comparable quality to the coated fibers and are therefore preferred.

The X-ray maps of Figs. 9 and 13 also help the understanding of the interface between the ceramic and the brazing alloy. The interface layer (3.5–4.0 μm) for the case without fibers (Fig. 9) was thicker than that (1.5–2.0 μm) for the case with fibers (Fig. 12). This is because a certain amount of titanium was segregated on the carbon fiber surface. If we allow the disappeared part of the Ti-rich band to deposit on the carbon fiber surface, a simple calculation shows that there should be a Ti-rich layer of thickness at least 0.3 μm thick on the carbon fiber surface. This value is consistent with the experimental results shown in Fig. 12(f). Although, in the case with carbon fibers, there was less Ti at the ceramic/braze interface, the interface bonding remained good. A smaller amount of Ti at the ceramic/braze interface is attractive as it limits the reaction between the ceramic and the braze, and the product is brittle.

Figure 11 reveals a notch at the ceramic/braze interface. The Ti X-ray map (Fig. 12(f)) shows segregation of titanium at the notch. This means that the ceramic/braze reaction was enhanced at the notch. A similar notch was also observed in Fig. 4(b), suggesting that the notch was where the first crack of the ceramic occurred during shear testing. Thus, a rough ceramic surface may degrade the strength of the joint.

Comparison of the top and bottom regions of Fig. 3 shows that the steel/braze interface (15–20 μm thick) was much thicker than the ceramic/braze interface (1.5–2.0 μm thick). Moreover, the microstructure of the steel/braze interface was less uniform that that of the ceramic/braze interface. Backscattered electron images of the steel/braze interfacial region (Fig. 11), along with the associated X-ray maps (Fig. 13), show that the molten braze aggressively attacked the steel, such that the elements in the steel reacted with the elements in the brazing alloy. The X-ray maps of Fe (Fig. 13(b)) and Ti (Fig. 13(d)) are similar at the steel/braze interface, suggesting that Fe–Ti inter-

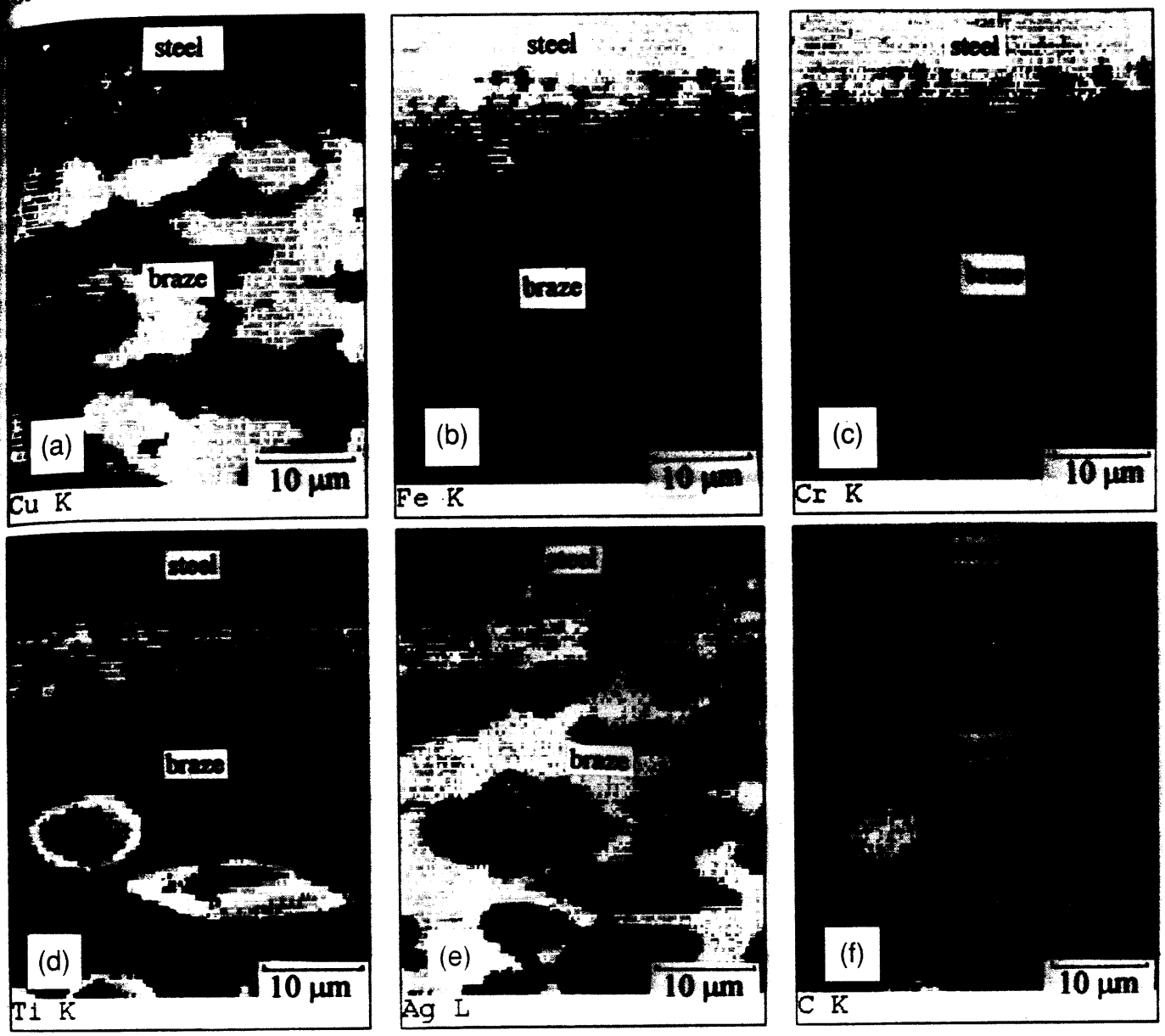

Fig. 13. X-ray maps for several elements in the region shown in Fig. 11.

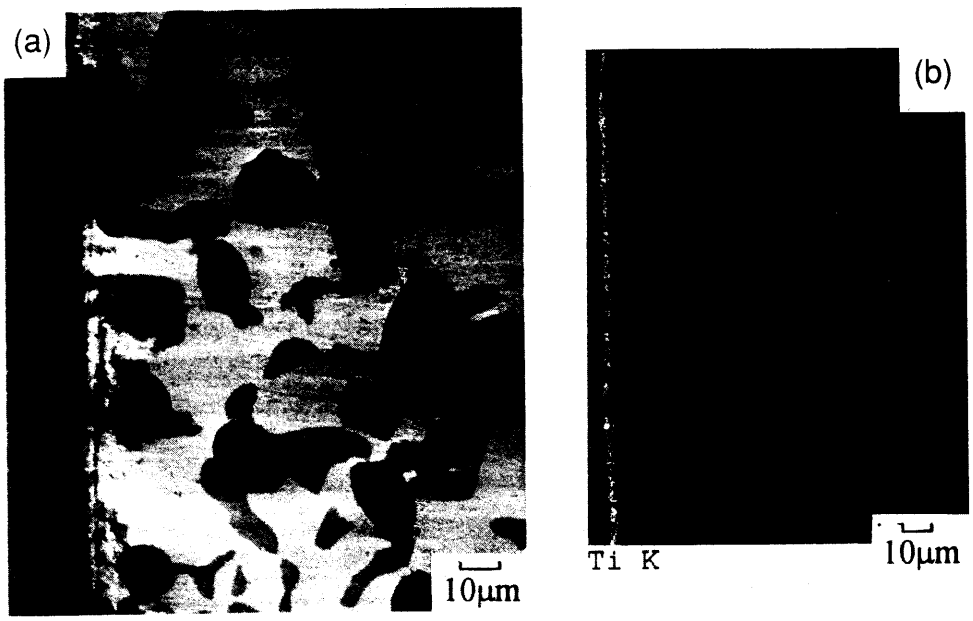

Fig. 14. (a) SEM backscattered electron image of the brazing layer with bare carbon fibers. (b) Ti X-ray map in the area shown in (a).

metallic compounds were probably formed. Since intermetallic compounds usually have low CTE and are brittle, they may contribute to the properties of the joint. Work is needed to identify these phases and control their formation.

The Ni and Cr elemental X-ray maps (Figs. 9(c) and (f)) show that these elements were dissolved from the steel into the brazing alloy. This means that the composition (and thereby the properties) of the brazing alloy was different from that before brazing. Considering these effects will help further development of brazing alloys for metal–ceramic joining.

IV. Conclusion

A composite active brazing material was developed. With the addition of 8.4 vol% short copper-coated carbon fibers, the debonding shear strength of alumina/steel joints increased by 18% for the case of uniformly distributed fibers and 28% for the case of fibers that were concentrated near the ceramic side of the ceramic/metal joint. In the latter case, the debonding occurred in the part of the brazing layer containing fewer fibers. The carbon fibers helped to strengthen the brazing alloy and decrease the thermal stress at the brazing interface. The titanium in the active brazing alloy was concentrated at the ceramic/braze, steel/braze, and carbon fiber/braze interfaces after brazing. If the brazing layer contained carbon fibers, the Ti-rich band at the ceramic/braze interface was thinner than in the case without carbon fibers. The copper coating on the carbon fibers disappeared from the carbon fiber surface after brazing and was replaced by Ti and Cr. Similar Ti segregation at the fiber–matrix interface was observed for the case of bare carbon fibers, which gave joints similar in quality to the copper-coated carbon fibers. The carbon fibers also served to lower the cost of the brazing material.

References

[1]R. E. Loehman and A. P. Tomsia, "Joining of Ceramics," *Am. Ceram. Soc. Bull.*, **67** [2] 375–80 (1988).
[2]M. G. Nicholas and D. A. Mortimer, "Ceramic Metal Joining for Structural Applications," *Mater. Sci. Technol.*, **1**, 657–65 (1985).
[3]J. R. McDermid and R. A. L. Drew, "Thermodynamic Brazing Alloy Design for Joining Silicon Carbide," *J. Am. Ceram. Soc.*, **74** [8] 1855–60 (1991).
[4]H. Mizuhara and K. Mally, "Ceramic-to-Metal Joining with Active Brazing Filler Metal," *Welding J.*, **64** [10] 27–32 (1985).
[5]J. Cao and D. D. L. Chung, "Carbon Fiber Silver–Copper Brazing Filler Composites for Brazing Ceramics," *Welding J.*, **71** [1] 21–24 (1992).
[6]W. Weise, W. Malikowski, and W. Bohn, "Active Brazing Alloys Make Strong, Economical Joints," *Ceram. Ind.*, **134** [2] 38–39 (1990).
[7]"Metz Brazing Products for Quality Metal Joining," Production Catalog, Metz Metallurgical Corp., South Plainfield, NJ, 1991.
[8]Technical conversation with R. J. Mulford, Braze Materials Product Manager, Degussa Corp., 1991.
[9]B. C. Coad, U.S. Pat. No. 4 409 181, 1983.
[10]A. L. Geiger and M. Jackson, "Low-Expansion MMCs Boost Avionics," *Adv. Mater. Proc.*, **136** [1] 23 (1989).
[11]D. D. L. Chung, *Carbon Fiber Composites*: Ch. 7. Butterworth-Heinemann, in press.
[12]K. Suganuma and T. Okamoto, "Interlayer Bonding Methods for Ceramic/Metal Systems with Thermal Expansion Mismatches," *Stud. Phys. Theor. Chem.*, **48**, 71–88 (1987).
[13]G. Economos and W. D. Kingery, "Metal–Ceramic Interactions: II, Metal–Oxide Interfacial Reactions at Elevated Temperature," *J. Am. Ceram. Soc.*, **36** [12] 403–409 (1953).
[14]P. R. Kapoor and T. W. Eagar, "Oxidation Behavior of Silver- and Copper-Based Brazing Filler Metals for Silicon Nitride/Metal Joints," *J. Am. Ceram. Soc.*, **72** [3] 448–54 (1989).
[15]T. Lyman (Ed.), *ASM Metals Handbook*. Vol. 6, *Welding, Brazing and Soldering*, 9th ed. American Society for Metals, Metals Park, OH, 1983.
[16]J. H. Selverian and S. Kang, "Ceramic-to-Metal Joints Brazed with Palladium Alloys," *Welding J.*, **71** [1] 25–33 (1992). □